CrossMark

RESEARCH ARTICLE

# Water-soluble ions and carbon content of size-segregated aerosols in New Delhi, India: direct and indirect influences of firework displays

Pawan Kumar[1] · Rakesh Kumar[1] · Sudesh Yadav[1]

**Abstract** The particle size distribution and water-soluble inorganic ion (WSII) and carbonaceous species in size-segregated aerosols, $Dp < 0.95$, $0.95 < Dp < 1.5$, $1.5 < Dp < 3.0$, $3.0 < Dp < 7.2$, and $7.2 < Dp < 10$ μm, were investigated during Diwali firework displays in New Delhi, India. The firework activity had the maximum contribution to the mass loading of $PM_{0.95}$ (786 μg/m$^3$) followed by $PM_{0.95-1.5}$ (216 μg/m$^3$) with all other three fractions accounting to a total of 214 μg/m$^3$. The percentage contributions of WSII to the total mass of aerosols were highest in first two size fractions (39 and 40 %, respectively), compared to other fractions. The firework marker ion ($Mg^{2+}$, $Cl^-$, and $K^+$) mass concentration shows higher values in $PM_{0.95}$ during Diwali compared to before Diwali period. The mass size distribution of particles, $NH_4^+$, $K^+$, $Cl^-$, $SO_4^{2-}$, $Mg^{2+}$, and $NO_3^-$, also showed changes on the Diwali night compared to previous and after days. The high $Cl^-/Na^+$ (5.6) and OC/EC (3.4) ratio of $PM_{0.95}$ can be used as the indicators of firework displays. The lowering of mixing height on Diwali night to 50 m compared to before (277 mts) and after (269 mts) Diwali period further concentrated the aerosols in ambient atmosphere. Therefore, the firework display not only released the gaseous or elemental constituent but also influenced the temperature profile and both put together result in high aerosol concentrations, WSII, OC, and BC contents in ambient atmosphere. The alveolar, respirable, and inhalable fractions accounted for 64.6, 90.8, and 97.8 %, respectively, of the total $PM_{10}$ mass. People stay exposed to such high pollution level in short span of 6–8 h and experience adverse health impacts due to high mass concentrations and the chemical components of fine aerosols.

## Introduction

The firework displays mark all important festivals, new year celebrations, or other important events such as Olympic games and commonwealth games (New Year's Eve celebrations, the Las Fallas in Spain, the Lantern Festival in China, Bonfire Night in the UK, Tihar in Nepal, Day of Ashura in Morocco, Skyfest in Ireland, Bastille Day in France) across the word. India, a "land of festivals," does have a tradition of major firework display to celebrate, Diwali, the festival of lights, every year during October or November that is attended by millions of people throughout the country. This anthropogenic activity taking place at different occasions and spanning over few hours time (4–6 h) is being widely studied for its influence on ambient air quality (Sarkar et al. 2010; Ambade and Ghosh 2013; Ganguly 2015; Kong et al. 2015 and references therein). Large quantities of firecrackers and sparkles are burnt during the festival to show the influence to the individuals (Tandon et al. 2008). Firecrackers contain chemicals such as potassium nitrates, potassium chlorate, potassium perchlorate, charcoal, sulfur, manganese, sodium oxalate, aluminum and iron dust powders, strontium nitrate, and barium nitrate for imparting colors, lightening, and energy source (Attri et al. 2001; Wang et al. 2007). Emissions generated from firework displays have attracted attention of scientists due to health impacts associated with them (Hirai et al. 2000; Limaye and Salvi 2010; Yang et al. 2014), visibility

✉ Sudesh Yadav
 sudesh27@hotmail.com

[1] School of Environmental Sciences, Jawaharlal Nehru University, New Delhi 110067, India

reduction (Wang et al. 2007; Kong et al. 2015), and formations of secondary pollutants (Attri et al. 2001).

The large amounts of soot, metal oxide particles, and precursors gases such as $SO_2$ and $NO_2$ emitted from firework display in short span of few hours catalyze the atmospheric reactions and processes for secondary particle formation (Jaing et al. 2015 and references therein). Attri et al. (2001) have reported formation of ozone during the firework display time on the night of Diwali festival in Delhi region. The airborne particles and gaseous constituents induced during and after the firework display have a unique chemistry and different compositions from the typical urban aerosols which need to be investigated. The previous works in India on air quality during firework displays had remained focused on gaseous pollutant and $PM_{10}$ chemistry (Attri et al. 2001; Ravindra et al. 2003; Sarkar et al. 2010; Perrino et al. 2011; Mandal et al. 2012; Nishanth et al. 2012; Chatterjee et al. 2013; Deka and Hoque 2014). The mass loading of size-segregated aerosols during firework displays has been studied by Tiwari et al. (2012) and Nishanth et al. (2012). In the light of the enhanced capabilities of collection and characterization of size-segregated aerosols, this work on size-segregated aerosols (≤0.95, 0.95–1.5, 1.5–3.0, 3.0–7.2, and 7.2–10 μm) was planned to investigate the influence of firework display on aerosols and soluble ion mass concentrations and carbon content.

## Experiments and methods

### Sampling site

The present study was carried out at the roof top of School of Environmental Sciences (SES), Jawaharlal Nehru University (JNU), New Delhi which is a residential academic institution located on the famous Delhi ridge with vast vegetation cover. Delhi, located in tropical climate zone (28° 35′ N; 77° 12′ E, 218 m MSL) and the capital city of India, is one of most polluted city of the India. Yamuna River flows across the city in the east side and the west is the fringe parts of the Thar Desert. The winters are characterized by low intensity NW winds and closed atmospheric conditions with temperature varying between 0 and 10 °C and relative humidity close to 100 %. Three coal-based thermal power plants (combined capacity ~1100 MW) and vehicular emissions are the major sources of air pollution in Delhi. In 2011–2012, the vehicular population was approximately 7.5 million (Economic Survey of Delhi 2012, 2013). A recent study by Yadav et al. (2016) in Delhi has reported contributions of different sources for $PM_{10}$ as crustal materials (21 %), industrial and vehicular emissions (23 %), and wind assisted transport and re-suspension of surface dust (56 %). The sampling site has very minimal emissions of pollutants at its own but acts as a receptor site for

pollutant from the nearby regions (Tandon et al. 2010; Kumar et al. 2014).

### Sample collection

Size-segregated aerosol samples were collected using mass flow controlled $PM_{10}$ high volume air sampler (Model TE-6070, Tisch Environmental Inc., USA) fitted with Cascade Impactor, (Model TE-236 of Tisch Environmental Inc., USA), which segregates the $PM_{10}$ in different size ranges. The aerosol samples were collected before Diwali [BF] (Nov. 3, 2010–Nov. 4, 2010), during Diwali [DF] (Nov. 5, 2010), and after Diwali [AF] (Nov. 6, 2010–Nov. 7, 2010) to capture the influence of episodic event of firework display on the occasion of Diwali festival in north India. The sampling duration for each sample was 24 h except for the Diwali period sampling which was six hourly. Each sample set comprised five aerosol samples in different size fractions. The cutoff diameters of the different stages of High Volume Cascade Impactor sampler were stage 1 Dp ≤ 0.95 μm (backup filter), stage 2 0.95 ≤ Dp ≥ 1.5 μm, stage 3 1.5 ≤ Dp ≥ 3.0 μm, stage 4 3.0 ≤ Dp ≥ 7.2 μm, and stage 5 7.2 ≤ Dp ≥ 10 μm. Aerosol samples were collected on quartz fiber filters (QFFs); four slotted/perforated filters (5.7 × 5.7 cm size) were used as impaction substrates for the collection of four coarser size fractions and one backup filter (20 × 25 cm size ) for the finest size fraction (stage 1). The QFFs were combusted at 550 °C for 6 h before use. The filter papers before and after sampling were conditioned for 24 h at 20 ± 1 °C and 50 ± 5 % relative humidity before weighing. The instrument was fitted with a mass flow controller and recorded real-time air volume concentration in cubic meter units. Field blank filters were also collected in each month by exposing filters in the sampler but not drawing air through them and were used to account for any artifacts introduced during the sample collection and handling procedure. The loss of quartz fibers during loading and unloading of the quartz filter papers of both sizes (5.5 cm × 5.6 cm and 20 cm × 25 cm) was monitored in the field blank samples and was found to be negligible.

The weight differences in the filter papers after and before the sampling was divided by the actual amount of air sucked in cubic meter units to calculate the mass concentrations of each size fraction of aerosols in μg m$^{-3}$. An electronic balance (Mettler Toledo, Model no. AB265-S/FACT) with accuracy of 0.01 mg was used for all weighing purposes throughout the study.

### Extraction and measurement of water-soluble ions

Water-soluble inorganic ion (WSII) species were extracted from each sample filter paper in 20 ml of ultra-pure Milli Q water using ultrasonic shaker maintained at room temperature. All the extraction solutions were filtered using a filter paper

(pore size 0.2 μm) and stored in high-density polyethylene (HDPE) bottles in the refrigerator at 4 °C until analysis. The Metrohm ion chromatograph (IC) model 882 Compact IC plus 1 pro 1 equipped with conductivity channel was used for analysis of major cations ($Ca^{2+}$, $Mg^{2+}$, $Na^+$, $K^+$, and $NH_4^+$) and anions ($F^-$, $Cl^-$, $NO_3^-$, and $SO_4^{2-}$) (Yadav and Kumar 2014).

## Carbon content analysis of $PM_{0.95}$

A 0.5-$cm^2$ punch from the filter was analyzed for eight carbon fractions following the IMPROVE_A thermal/optical reflectance (TOR) protocol on a DRI model 2001 carbon analyzer (Atmoslytic Inc., Calabasas, CA) (Cao et al. 2007; Chow et al. 2007). The analyzer works on preferential oxidation of organic carbon and elemental carbon at different temperatures. This produced four organic carbon (OC) fractions (OC1, OC2, OC3, and OC4 at 140, 280, 480 and 580 °C in a helium [He] atmosphere), OP (a pyrolyzed carbon fraction), and three elemental carbon (EC) fractions (EC1, EC2, and EC3 at 580, 740, and 840 °C in a 2 % $O_2$ and 98 % He atmosphere), wherein the corrected EC1 is equal to EC1 minus OP. This corrected EC1 will be the one referred to as "EC1 fraction" in this work. The IMPROVE_TOR OC is operationally defined as OC1 + OC2 + OC3 + OC4 + OP and EC is defined as EC1 + EC2 + EC3 − OP (Chow et al. 2007). The EC is further divided into char (EC1 − OP) and soot (EC2 + EC3) (Han et al. 2009). The instrument performance was checked against the internal standards after the analyzing every 10 samples. All the reported concentrations were corrected for laboratory and field blanks.

## Quality assurance and quality control

All the physical measurements, sample extraction and storage, and WSII analysis on Metrohm IC were carried out at SES, JNU, New Delhi in a metal free positive pressure clean laboratory having 1000 class air flow in lab and 100 class air flow in the fume hood. All filter papers handling was done with high quality plastic forceps.

The efficacy of the water-soluble extraction protocol was checked by re-extracting ions from the previously used sample filter papers in the same manner and extraction efficacy (in % units) which was recorded in the range of 90–100 %. The average recoveries of ions from quartz filter papers were found in the range of 92–100 %.

The accuracy and precision were within 5 %, whereas recovery was found to be varied between 96 and 100 %. The instrument performance was checked against the working standards after every five samples, and if the recovery was not found within the range, then the instrument was re-calibrated. The field blank levels were calculated by following same procedure, averaged, and subtracted from the sample

measurements The quality assurance and control are discussed in detail in our previous works (Kumar and Yadav 2013; Yadav and Kumar 2014).

## Meteorological data

The meteorological parameters viz relative humidity, dew point temperature, wind direction, wind speed, events, and mixing height for the sampling period were taken from the automatic weather station installed on the roof top of the building adjacent to the sampling site in JNU and from Air Resources Laboratory: National Oceanic and Atmospheric Administration (ARL-NOAA) (http://www.arl.noaa.gov/) and are provided in Table 1.

## Results and discussions

### Mass concentration of size-segregated aerosols

The mean mass concentrations along with standard deviation (SD) of five different size fractions collected BF, DF, and AF periods are given in Table 2. The percentage contribution of each size fractions to their total sum ($\sum PM_{10}$) is also provided in Table 2. The $\sum PM_{10}$ mass concentrations in BF, DF, and AF periods were observed as 354, 1216, and 399 μg $m^{-3}$, respectively, and were much higher than that observed by Chatterjee et al. (2013) at Kolkata (711 μg $m^{-3}$) and Nirmalkar et al. (2013) at Rajim, Chhattisgarh (556 μg $m^{-3}$) during similar events and exceeded the national ambient air quality standards value of 60 μg $m^{-3}$ for 24 h average (CPCB, New Delhi). At the time of firework display, i.e., DF, the $PM_{0.95}$ mass concentration reached as high as 786 μg $m^{-3}$ showing an increase of ~4 times compared to BF period (183 μg/$m^3$), an observation similar to Joly et al. (2010). Similar size distribution and contribution of $PM_1$ have been observed during Chinese Spring Festival in Lanzhou, northwestern China by Zhao et al. (2014).

The $PM_{1.5}$ ($PM_{0.95}$ + $PM_{0.95–1.5}$) contribution to the total $PM_{10}$ load was found to be 62, 83, and 81 % in BF, DF, and, AF periods, respectively. The smaller percentage contribution of $PM_{1.5–10}$ mass compared to $PM_{0.95}$ to the $PM_{10}$ during firework displays suggested that more of $PM_{0.95}$ is generated during firework activity. This is clear from Table 2 that the other fractions have limited contributions to $PM_{10}$. This is attributed to the emissions of finer aerosols ($PM_{1.5}$) due to burning of fire crackers which further got enhanced on account of calm meteorological conditions (low wind speeds and low mixing heights) (Table 1). The mass concentrations of five different size fractions of aerosols collected before, after, and during Diwali are plotted in Fig. 1.

The particle mass size distribution in BF period follows the pattern of typical urban aerosols, i.e., bimodal. The finer mode

**Table 1** Meteorological parameters during the Diwali firework period in Delhi

| | Before Diwali (BF) | During Diwali (DF) | After Diwali (AF) |
|---|---|---|---|
| Temperature (°C) | 22 | 19.4 | 22.7 |
| Dew Point (°C) | 13.1 | 16.2 | 15.4 |
| Humidity (%) | 59.8 | 83.1 | 66.3 |
| Sea level pressure (hPa) | 1015 | 1013 | 1013.3 |
| Visibility (Km) | 1.3 | 0.5 | 1.1 |
| PBL (mts)[a] | 227 | 47 | 269 |
| Wind direction | W, NNW, NE | Calm | W, WNW |
| Wind speed (Km/h) | 3.4 | Calm | 2.4 |
| Events | | Fog | |

[a] Planet boundary layer (PBL) data is taken from Air Resources Laboratory (ARL) of the National Oceanic and Atmospheric Administration (NOAA)

is attributed to vehicular (people travel a lot during BF and AF periods) and local biomass burning as well as to air mass transport from the biomass burning in adjoining states of Haryana and Punjab (Singh and Kaskaoutis 2014) during the month of November, and the coarser mode is attributed to local fine aerosols and re-suspension activity (Gargava et al. 2014). The particle mass size distribution changes in DF and AF period due to continuous emissions on DF period, as well as citywide sweeping (Tandon et al. 2008) and the secondary aerosol formation mechanisms in AF periods. The firework-induced particles remain in suspension in air for long periods, from days to weeks under prevailing meteorological conditions (Kong et al. 2015).

## WSII variations in BF, DF, and AF periods

The data on the concentrations of water-soluble inorganic ions (WSIIs) in different size fractions of aerosols collected BF, AF, and DF are given in Table 3. The calculated ratio of total anions to total cations for the DF period were found to be 1.25, 1.33, 1.01, 1.11, and 0.86 for stages 1, 2, 3, 4, and 5 aerosols, respectively, and indicated a cation deficient condition except for stage 5. This lack of cations can be explained due to the abundance of soluble transition metals, such as $Al^{3+}$, $Pb^{2+}$, $Cu^{2+}$, $Mn^{2+}$, $Sr^{2+}$, and $Zn^{2+}$, which are used as additives in the fireworks (Wang et al. 2007) but were not analyzed in this work. The stage five ($PM_{7.2–10}$) largely contains the crustal

mass and least firework imprints and, therefore, does not show cation deficiency. The value of 0.86 for stage 5 samples is so because bicarbonate analysis was not performed, whereas the crustal material in this region does contain the soluble carbonates and bicarbonates (Kumar and Yadav 2016). The percentage contributions of each individual ion to the total sum of all ions in size fractionated aerosols collected during firework display in different time periods are given in Fig. 2a–o.

The WSII in $PM_{0.95}$ of DF period shows the order of abundance as $SO_4^{2-} > K^+ > NO_3^- > Cl^- > Mg^{2+} > NH_4^+ > Na^+ > Ca^{2+} > F^-$ (Fig. 2f). The concentrations of all ionic species during DF periods were higher than those during the BF and AF periods except for $NH_4^+$. Among the ionic species, $Mg^{2+}$ (4.43 µg m$^{-3}$), $Cl^-$ (19.68 µg m$^{-3}$), and $K^+$ (113.40 µg m$^{-3}$) of $PM_{0.95}$ sampled in DF periods were considerably higher than samples of BF and AF periods. The concentrations of $Mg^{2+}$, $Cl^-$, and $K^+$ in $PM_{0.95}$ of DF periods were approximately 147.7, 89.5, and 26.3 times higher, respectively, compared to that in BF periods (Table 3).

The mass percentage contribution of the marker ions ($Mg^{2+}$, $Cl^-$, and $K^+$) of firework displays went up to 39 % in DF (Fig. 2f) compared to 15 % in BF (Fig. 2a). The percentage contribution of nitrate concentration did not increase during firework display which was in agreement with Vecchi et al. (2008), Drewnick et al. (2006), and Kong et al. (2015). The other point is that the secondary inorganic aerosols (SIA) ($NH_4^+$, $SO_4^{2-}$, and $NO_3^-$) showed higher values in AF

**Table 2** Aerosol mean mass concentrations (µg m$^{-3}$) of particles distributed through Dp (µm) intervals before, during, and after Diwali periods

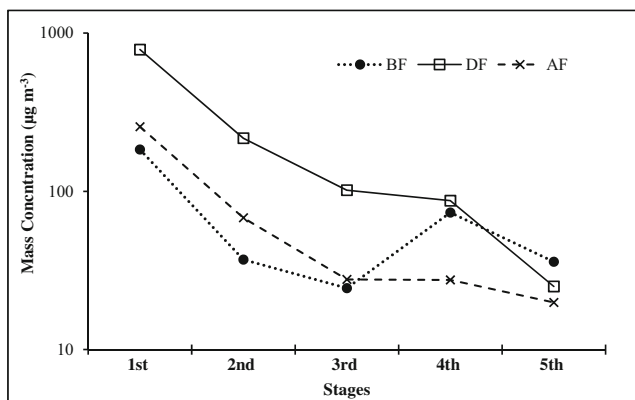| | $PM_{0.95}$ First stage | $PM_{0.95–1.5}$ Second stage | $PM_{1.5–3.0}$ Third stage | $PM_{3.0–7.2}$ Fourt stage | $PM_{7.2–10}$ Fifth stage | $\sum PM_{10}$ |
|---|---|---|---|---|---|---|
| Before Diwali (BF) | 183 ± 99 | 37 ± 99 | 24 ± 99 | 73 ± 99 | 36 ± 99 | 354 |
| % $\sum PM_{10}$ | 52 | 10 | 7 | 21 | 10 | |
| During Diwali (DF) | 786 ± 93 | 216 ± 45 | 102 ± 13 | 87 ± 18 | 25 ± 1 | 1216 |
| % $\sum PM_{10}$ | 65 | 18 | 8 | 7 | 2 | |
| After Diwali (AF) | 256 ± 83 | 68 ± 68 | 28 ± 9 | 28 ± 16 | 20 ± 6 | 399 |
| % $\sum PM_{10}$ | 64 | 17 | 7 | 7 | 5 | |

**Fig. 1** Mass size distribution of aerosols collected before Diwali (BF), during Diwali (DF), and after Diwali (AF) periods. Stages on the X axis are 1st stage $Dp \leq 0.95$ μm, 2nd stage $0.95 \leq Dp \geq 1.5$ μm, 3rd stage $1.5 \leq Dp \geq 3.0$ μm, 4th stage $3.0 \leq Dp \geq 7.2$ μm, and 5th stage $7.2 \leq Dp \geq 10$ μm

samples compared to DF. This suggested that the effect of firework activities remained on the chemical composition of finer fraction of aerosols collected even in AF period. The reduced fraction of SIA associated in the DF period was due to the lower amounts of $NH_4^+$ and $NO_3^-$ (Yang et al. 2014). The higher values of ratio (AF/BF) for $Mg^{2+}$, $Na^+$, $K^+$, and $Cl^-$ ion are associated to the re-suspension of fine aerosols carrying the imprints of tracer-source-specific elements of fireworks. Tandon et al. (2008) have reported that nearly 27 %

of ambient aerosols mass on account of citywide sweeping on the following morning of Diwali festival in Delhi. The contributions on account of wind-assisted re-suspension can be ruled out as the wind speed was lower (2.4 Km $h^{-1}$) during AF period compared to the BF period (3.4 km $h^{-1}$; Table 1). The molar ratio of $Cl^-$ to $Na^+$ ($Cl^-/Na^+$) in aerosols remains near unity in Delhi during the non-firework display periods (Kumar and Yadav 2016), but it increased to 5.6 during the DF periods. The $Cl^-/Na^+$ ratio of atmospheric fine particles can be used as the indicator of firework burning as observed by Tsai et al. (2012) during Taiwan's Lantern Festival.

The WSII in $PM_{0.95–1.5}$ of DF period shows the following order of abundance as $SO_4^{2-} > K^+ > Cl^- > NO_3^- > NH_4^+ > Mg^{2+} > Ca^{2+} > Na^+ > F^-$ and constituted 48 % of the total mass concentration (Fig. 2g). The concentrations of all ionic species during DF period were higher than AF periods. Among the ionic species, $Mg^{2+}$ (2.06 μg $m^{-3}$), $Cl^-$ (12.29 μg $m^{-3}$), and $K^+$ (26.34 μg $m^{-3}$) in $PM_{0.95–1.5}$ samples were higher than those observed in BF and AF samples. The concentrations of $Mg^{2+}$, $Cl^-$, and $K^+$ in DF period were higher by a factor of 34.4, 3.7, and 32.1, respectively, compared to their concentrations in BF samples. The percentage contributions of these marker ions ($Mg^{2+}$, $Cl^-$, and $K^+$) of firework displays went up to 40 % in total soluble ions in DF samples (Fig. 2g). The $NO_3^-$ and $NH_4^+$ concentrations in DF contributed to 11

**Table 3** Mass concentrations of water-soluble inorganic ions (μg $m^{-3}$), distributed through different particle diameter (Dp) aerosols collected before (BF), after (AF), and during Diwali festival time

|  | $F^-$ | $Cl^-$ | $NO_3^-$ | $SO_4^{2-}$ | $Na^+$ | $NH_4^+$ | $K^+$ | $Ca^{2+}$ | $Mg^{2+}$ | $\sum$Ions | PM | % Ions | $NO_3^-/SO_4^{2-}$ |
|---|---|---|---|---|---|---|---|---|---|---|---|---|---|
| $PM_{0.95}$ (first stage ) | | | | | | | | | | | | | |
| BF | 0.11 | 0.22 | 6.63 | 13.39 | 0.33 | 2.18 | 4.3 | 1.38 | 0.03 | 28.6 | 183 | 16 | 0.50 |
| DF | 1.24 | 19.68 | 31.80 | 172.11 | 2.28 | 3.20 | 113.4 | 1.46 | 4.43 | 349.6 | 786 | 44 | 0.18 |
| AF | 0.70 | 0.82 | 13.27 | 35.64 | 1.07 | 5.06 | 13.6 | 1.24 | 0.53 | 71.9 | 256 | 28 | 0.37 |
| $PM_{0.95–1.5}$ (second stage) | | | | | | | | | | | | | |
| BF | 0.04 | 3.28 | 4.23 | 2.33 | 0.14 | 1.81 | 0.8 | 0.52 | 0.06 | 13.2 | 37 | 36 | 1.82 |
| DF | 0.50 | 12.29 | 11.65 | 45.68 | 0.46 | 3.64 | 26.3 | 0.57 | 2.06 | 103.2 | 216 | 48 | 0.26 |
| AF | 0.39 | 3.45 | 12.07 | 11.51 | 0.13 | 4.06 | 4.9 | 0.40 | 0.34 | 37.3 | 68 | 55 | 1.05 |
| $PM_{1.5–3.0}$ (third stage) | | | | | | | | | | | | | |
| BF | 0.03 | 1.46 | 1.84 | 0.91 | 0.09 | 0.67 | 0.3 | 0.81 | 0.05 | 6.1 | 24 | 26 | 2.02 |
| DF | 0.26 | 4.90 | 4.02 | 16.96 | 0.20 | 1.31 | 10.2 | 0.90 | 1.06 | 39.8 | 102 | 39 | 0.24 |
| AF | 0.18 | 1.46 | 4.20 | 3.01 | 0.06 | 1.44 | 1.4 | 0.54 | 0.16 | 12.5 | 28 | 45 | 1.39 |
| $PM_{3.0–7.2}$ (fourth stage) | | | | | | | | | | | | | |
| BF | 0.05 | 2.28 | 5.08 | 1.66 | 0.27 | 0.60 | 0.3 | 1.99 | 0.14 | 12.4 | 73 | 17 | 3.06 |
| DF | 0.34 | 3.29 | 5.34 | 9.90 | 0.25 | 1.15 | 5.7 | 2.19 | 0.59 | 28.8 | 87 | 33 | 0.54 |
| AF | 0.24 | 1.53 | 5.24 | 1.80 | 0.13 | 1.17 | 0.8 | 1.37 | 0.13 | 12.4 | 28 | 45 | 2.91 |
| $PM_{7.2–10}$ (fifth stage) | | | | | | | | | | | | | |
| BF | 0.03 | 0.77 | 1.66 | 0.61 | 0.13 | 0.20 | 0.1 | 0.95 | 0.06 | 4.6 | 36 | 13 | 2.72 |
| DF | 0.18 | 1.01 | 1.95 | 1.81 | 0.07 | 0.70 | 1.1 | 0.90 | 0.12 | 7.8 | 25 | 31 | 1.08 |
| AF | 0.17 | 0.78 | 2.13 | 0.64 | 0.07 | 0.65 | 0.2 | 0.74 | 0.05 | 5.4 | 20 | 27 | 3.35 |

**Fig. 2** Percentage contribution of individual ions to total sum of all ions aersols collected before Diwali (*left column*), during Diwali (*middle column*), and after Diwali periods (*right column*). **a–e, f–j, k–o** represent the first stage $Dp \leq 0.95$ μm, second stage $0.95 \leq Dp \geq 1.5$ μm, third stage $1.5 \leq Dp \geq 3.0$ μm, fourth stage $3.0 \leq Dp \geq 7.2$ μm, and fifth stage $7.2 \leq Dp \geq 10$ μm, respectively
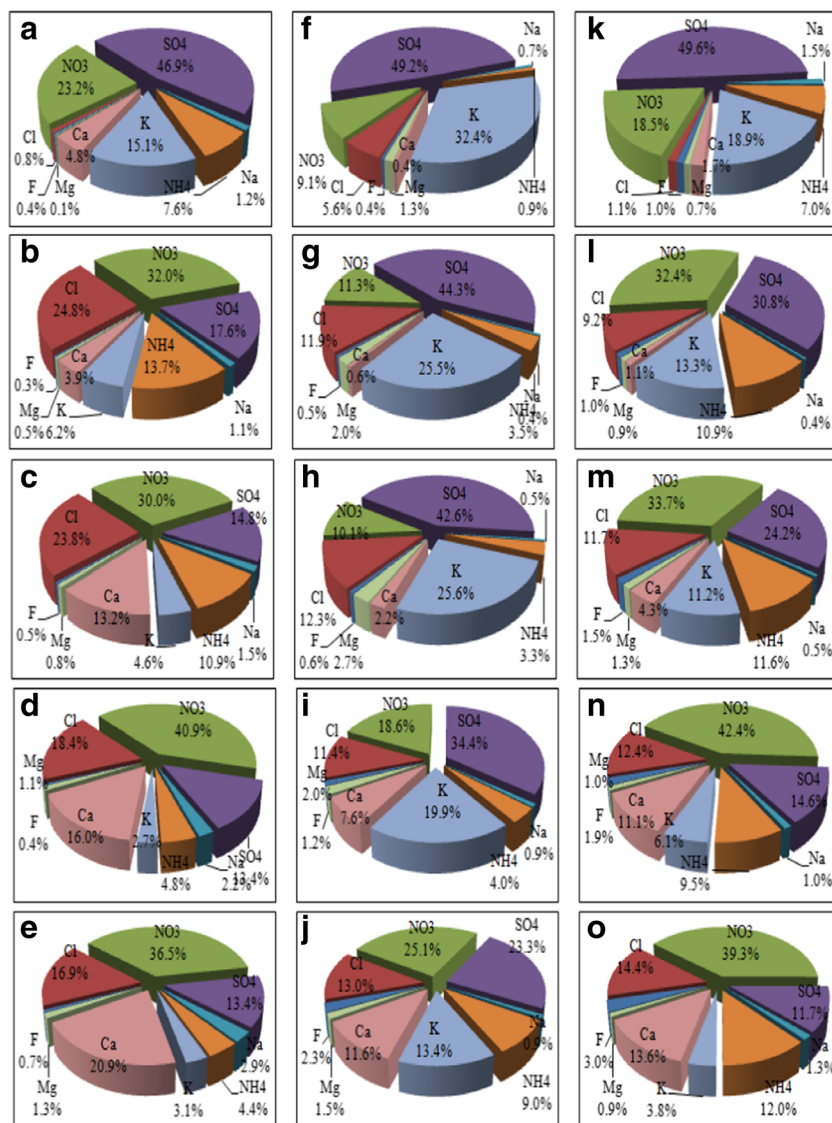


and 4 % (Fig. 2g) of the total WSII, but it increased up to 32 and 11 %, respectively, during AF (Fig. 2l). This indicates the formation of SIA from the emissions of firework displays after DF period.

The WSII in $PM_{1.5–3.0}$ of DF period followed the order of abundance as $SO_4^{2-} > K^+ > Cl^- > NO_3^- > NH_4^+ > Mg^{2+} > Ca^{2+} > F^- > Na^+$ and constituted 39 % of the total mass concentration (Table 3; Fig. 2h). Among the ionic species, $Mg^{2+}$ (1.06 μg m$^{-3}$), $Cl^-$ (4.90 μg m$^{-3}$), and $K^+$ (10.18 μg m$^{-3}$) of $PM_{1.5–3.0}$ sampled in DF periods were higher than those observed in BF and AF samples. The concentrations of $Mg^{2+}$, $Cl^-$, and $K^+$ during DF periods were 21.3, 3.4, and 36.4 times, respectively, which are higher than BF periods. The mass percentage contribution of these ions ($Mg^{2+}$, $Cl^-$, and $K^+$) to total WSII rose to 40 % in DF samples (Fig. 2h) compared to 29 and 24 % in BF and AF periods, respectively (Fig. 2c, m). The

$NO_3^-$ and $NH_4^+$ concentrations in DF samples constituted only 10 and 3 % (Fig. 2h) of total WSII, but it increased up to 33 and 9 % in BF and AF periods, respectively (Fig. 2c, m).

The WSII in $PM_{3.0–7.2}$ of DF period shows the following order of abundance as $SO_4^{2-} > K^+ > NO_3^- > Cl^- > Ca^{2+} > NH_4^+ > Mg^{2+} > F^- > Na^+$ and contributes 33 % of the total mass concentration (Table 3; Fig. 2i), which is relatively lower than the percentage contributions of all WSII to mass concentrations of stages 1, 2, and 3 (Fig. 2f–h). It suggests that WSIIs generated during firework are more concentrated in finer fraction of aerosols and contain more water-soluble ions. The concentrations of $Mg^{2+}$, $Cl^-$, and $K^+$ in DF periods were approximately 4.2, 1.4, and 16.8 times, respectively, higher than BF periods. The mass percentage contribution of these ions ($Mg^{2+}$, $Cl^-$, and $K^+$) rose to 33 %

during DF period (Fig. 2i) compared to 29 and 19 % during BF and AF periods, respectively (Fig. 2d, n).

The WSII in $PM_{7.2-10}$ of DF period shows the following order of abundance as $NO_3^- > SO_4^{2-} > K^+ > Cl^- > Ca^{2+} > NH_4^+ > F^- > Mg^{2+} > Na^+$ and contributes 31 % of the total mass concentration which is lowest percentage contribution (Table 3; Fig. 2j) of WSII among all size fractions (Fig. 2f–i). The mass concentration of $PM_{7.2-10}$ (25 µg m$^{-3}$) in DF period is lower than that in BF (36 µg m$^{-3}$). This suggests that firework-induced aerosols dominates only in the particle size range below 3 µm, and the particles in coarser size fractions are least affected by firework displays.

Sulfur and nitrogen in the atmosphere originate from both stationary and mobile sources. Arimoto et al. (1996) used the mass ratio of $[NO_3^-]/[SO_4^{2-}]$ as an indicator of relative importance of stationary versus mobile sources of sulfur and nitrogen in the atmosphere.

High $[NO_3^-]/[SO_4^{2-}]$ mass ratios indicate the predominance of mobile sources over the stationary source pollutants. In the present study, this ratio was found to be 0.3 for DF, indicating the dominance of stationary source as firework displays over mobile sources, which are more active in BF and AF periods. This is also reflected in the higher values of this ratio in all size range aerosols of BF and AF samples compared to DF samples (Table 3). Wang et al. (2007) have also reported the influence of firework activity on $NO_3^-$ and $SO_4^{2-}$ concentrations in aerosols.

### Size distribution of major WSII

The size distribution for major water-soluble ions ($NH_4^+$, $K^+$, $Cl^-$, $SO_4^{2-}$, $Mg^{2+}$, and $NO_3^-$) is shown in Fig. 3 during three different periods (BF, DF, and AF). All soluble ions showed highest concentrations in $PM_{0.95}$ fractions followed by



Fig. 3 Mas size distribution of major water-soluble inorganic ions in Diwali time sampling [before Diwali (BF); during Diwali (DF), and after Diwali (AF)]. Note that the number of stages on the X axis of each graph represents first stage Dp ≤ 0.95 µm, second stage 0.95 ≤ Dp ≥ 1.5 µm, third stage 1.5 ≤ Dp ≥ 3.0 µm, fourth stage 3.0 ≤ Dp ≥ 7.2 µm, and fifth stage 7.2 ≤ Dp ≥ 10 µm, respectively
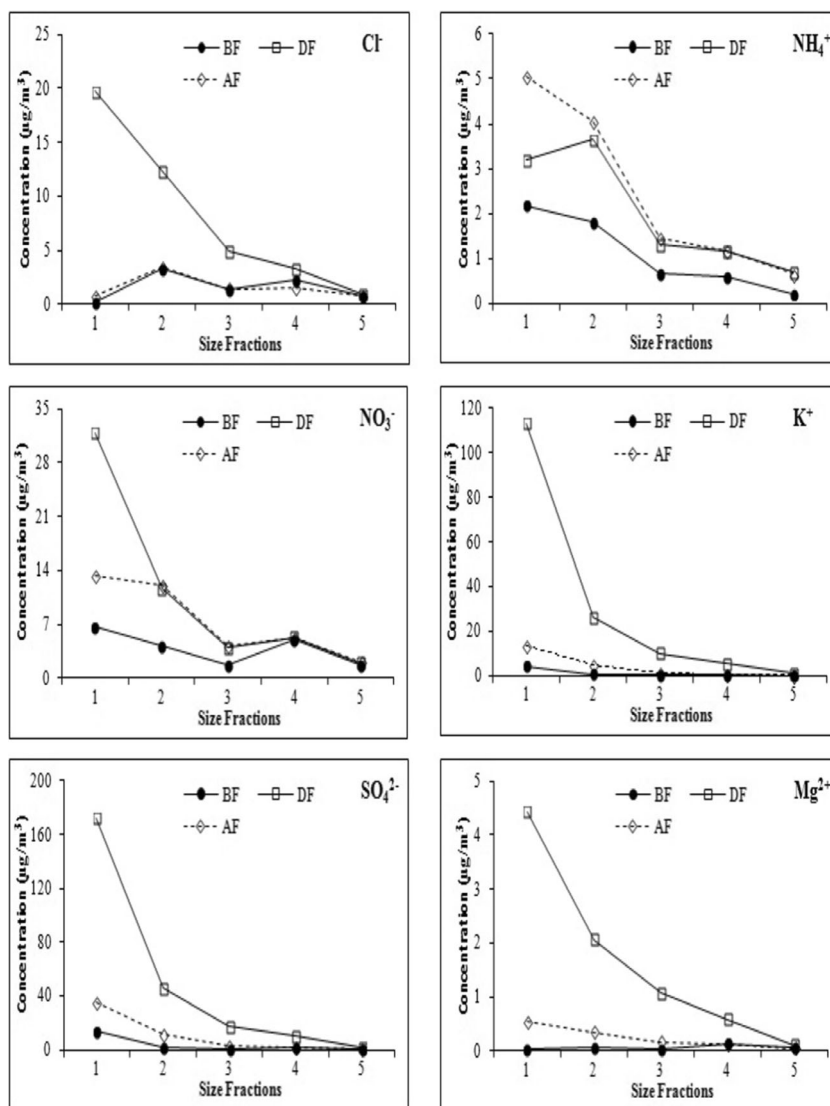
$PM_{0.95–1.5}$ fractions, whereas all other fractions have limited amounts of soluble ions. The $Cl^-$ and $NO_3^-$ showed bimodal distribution in BF and AF samples, but during DF period, $Cl^-$ ions follow a linear decrease from stage 1 to stage 5, and $NO_3^-$ ion still follow nearly bimodal with more enrichment in first stage fraction. This is indicative of single source (firework) for $Cl^-$ ions and two sources (firework and crustal dust) for $NO_3$ ions.

In general, it can be arrived at that all ions show unimodal distribution with highest concentrations in stage 1 ($PM_{0.95}$) aerosols which decrease in linear fashion until stage 3 and follow flat pattern afterward. The other information from Fig. 3 is that all soluble ions showed higher concentrations in DF followed by AF samples except that $Cl^-$ ions show similar concentrations and size distribution pattern in BF and AF samples. The size distributions for soluble ions ($K^+$ and $Mg^{2+}$) that are directly emitted by firework displays follow similar size distribution patterns compared to the ions ($NO_3^-$, $SO_4^{2-}$, $NH_4^+$) which are formed in the ambient atmosphere as secondary product. Variations in $Cl^-$ size distribution and concentration were in tune with $K^+$ ions and $Cl^-$ showed strong correlation with $K^+$ for all size fractions in DF samples. Thus, $Cl^-$ is also likely to be of primary origin as $K^+$ ions from firework displays.

## Carbonaceous materials in $PM_{0.95}$

Total carbon (TC = EC + OC) component in $PM_{0.95}$ aerosols over Delhi during firework displays was 145.99 $\mu g\ m^{-3}$. The TC was dominated by OC (115.75 $\mu g\ m^{-3}$) in comparison to EC (30.24 $\mu g\ m^{-3}$) in DF samples and was about 2.6 and 1.8 times higher than that observed in BF and AF samples, respectively (Table 4).

In Delhi, generally OC content dominates over the EC content in all seasons (Kumar and Yadav 2016). The EC fraction for DF is higher than BF and AF periods as also previously observed by Sarkar et al. (2010). This increase in EC on Diwali day indicates the contributions from firework burnings. Charcoal, used in fireworks, could possibly be a reason for high EC during Diwali day (Wang et al. 2007). This is further supported by the higher EC1 (char EC 26.66 $\mu g\ m^{-3}$) compared to less than 1 $\mu g\ m^{-3}$ concentrations of EC2 and EC3 in DF samples. The EC2 and EC3, marked as soot EC, are formed due to high temperature burning of fossil fuel, and limited vehicular activity on DF period is a possible reason for that as people stay at home during the festival night. Soot EC (EC2 + EC3) was higher (in only relative terms as the concentrations remained less than 1 $\mu g\ m^{-3}$) in DF period compared to BF and AF periods due to its limited direct emissions from firework displays as has also been observed by Do et al. (2012).

**Table 4** Organic carbon (OC) and elemental carbon (EC) concentrations ($\mu g\ m^{-3}$ units) in $PM_{0.95}$ collected during Diwali festival time in Delhi

|  | Before Diwali (BF) | During Diwali (DF) | After Diwali (AF) |
|---|---|---|---|
| OC1 | 0.02 | 0.25 | 0.17 |
| OC2 | 18.21 | 24.28 | 12 |
| OC3 | 13.06 | 31.28 | 16.06 |
| OC4 | 1.21 | 5.23 | 3.87 |
| EC1 | 13.6 | 26.66 | 20.22 |
| EC2 | 0.36 | 0.71 | 0.53 |
| EC3 | 0.06 | 0.37 | 0.19 |
| OP | 14.28 | 33.2 | 13.31 |
| OC | 47 | 94 | 45 |
| EC | 14 | 28 | 21 |
| TC | 61 | 122 | 66 |
| $PM_{0.95}$ | 183 | 786 | 256 |
| TCM[a] | 90 | 181 | 96 |
| % TCM | 49 | 23 | 37 |

[a] TCM = organic matter (OM) + elemental matter (EM); OM = 1.6 × OC and EM = 1.1 × EC

Among the OC fractions, OC2 and OC3 were dominant contributors with limited amounts of OC1 and small amount of OC4. Therefore, it can be arrived at that firework displays add OC2, OC3, and EC1 to the carbon fraction in $PM_{0.95}$ in the ambient atmosphere. The before Diwali sample showed considerable concentrations of OC and EC, which may be due to high influx of traffic from neighboring regions into Delhi during this time for festival shopping and biomass burning prevalent in adjoining states of Punjab and Haryana (Singh and Kaskaoutis 2014). The AF period concentrations of OC and EC are linked to re-suspension of deposited emissions of firework displays on preceding night.

High OC/EC ratio value of 3.4 could be used as possible signature for firework displays. The decrease in OC/EC ratio in AF period is indicative of the fact that the direct emission of firework displays has ceased and the contributions of diesel vehicle exhaust started showing up as well as photochemistry-based production of secondary organic aerosols (Feng et al. 2012).

The total carbonaceous material (TCM) was estimated as follows after Yttri et al. (2007):

$$TCM = organic\ matter(OM) + elemental\ matter(EM)$$

where OM = 1.6 × OC and EM = 1.1 × EC.

For conversion of OC to OM, a wide range of values (1.2 to 2.1) has been reported (Turpin and Lim 2001), but a value of 1.6 has been used for the urban aerosols (Cao et al. 2003). To calculate EM from EC, a conversion factor of 1.1 was used after Kiss et al. (2002). The TCM accounted for 49, 23, and

37 % in BF, DF, and AF samples, respectively (Table 4). The high percentage contribution of TCM in AF is associated with aging mechanism, i.e., formation of secondary organic aerosols (Feng et al. 2012). Higher TCM in BF samples are directly linked to the sources as there are large traffic inflows and movements across the city as people greet each other and do shopping, whereas people stay at home for festival celebrations during DF period.

### Health risk assessment

The airborne particles enter into the human body through breathing and finally reach to different body parts based on their aerodynamic diameter. The distribution of particles and chemical constituents in three major fractions, alveolar (<0.95 μm), respirable (<3.0 μm), and inhalable (<7.2 μm) was calculated according to O'Shaughnessy and Raabe (2003) and is shown in Fig. 4. The inhalable fraction represents particles of an aerodynamic diameter that can enter the nose and/or mouth during breathing. The respirable fraction contains particles of aerodynamic sizes that can penetrate beyond larynx and enter into lungs, and the alveolar fraction of aerosol contains particles of aerodynamic sizes that can penetrate into the gas exchange regions of the lungs (the alveolar region).

The alveolar, respirable, and inhalable fractions accounted for 64.6, 90.8, and 97.8 %, respectively, of the total $PM_{10}$ mass. The major WSII exhibited significant abundance in these fractions. It is important to note that alveolar fraction is more dominant than the other two fractions and always constituted more than 50 % of the other two fractions. The results hint that serious health implications can emerge, more so in case of children, old age persons, and those already suffering from
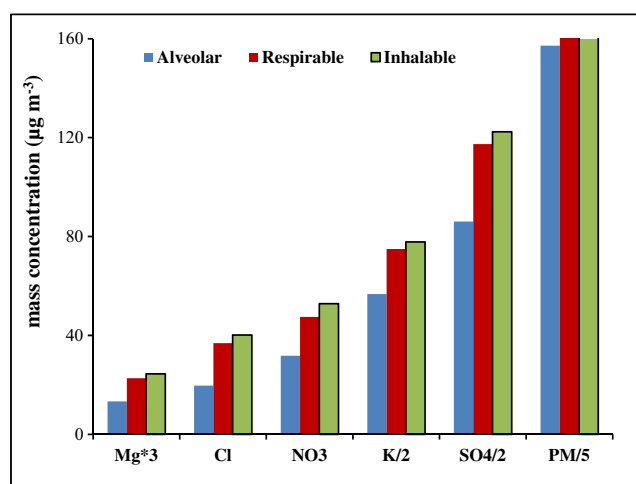


**Fig. 4** Distribution of soluble ions and particulate matter in alveolar (<0.97 μm), respirable (<3.0 μm), and inhalable (<7.2 μm) fractions during firework display at Delhi. The concentrations of $K^+$, $SO_4^{2-}$, and $PM_{10}$ are divided by a factor of 2, 2, and 5 and $Mg^{2+}$ is multiplied by 3 to bring the values in scale

breathing or other diseases, even though people are exposed to such emission for a limited period. Recently, Ganguly (2015) have reported that firework activity indirectly influences the survival rates of viruses responsible for viral infections resulting in sudden hike in respiratory infections during the festival. It is suggested either to reduce the firework activity or to wear the mask fitted with air filter during the firework activity to safe guard the human health from direct and indirect effects of this activity.
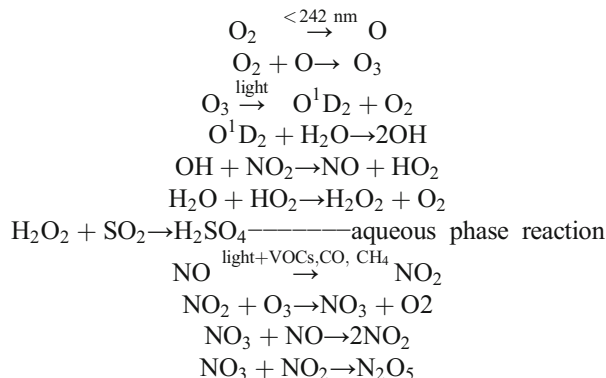
### Discussions

The results of this study indicated that firework displays play three different roles in the aerosols mass concentrations and their soluble ion characteristics. First, the firework displays is a potential source of $PM_{0.95}$ fraction followed by $PM_{0.95–1.5}$ and $PM_{1.5–3.0}$ in the ambient atmosphere. The high concentrations could be on account of direct emissions of particles during this activity. Higher $Mg^{2+}$ concentrations are due to its use as metallic fuel in fireworks for color and brightness (Wang et al. 2007; Chatterjee et al. 2013). The high $Cl^-$ concentration was due to the fact that oxidizers used in the firecrackers are salts of chlorates and per chlorates. Potassium salts such as nitrates, chlorates, and per chlorates are widely used as oxidizers in fireworks. The chemical equations which explain the formations of soluble salts of chloride and potassium during firework displays (Wang et al. 2007) can be written as $2KNO_3 = 2KNO_2 + O_2$, $2KClO_3 = 2KCl + 3O_2$, and $KClO_4 = KCl + 2O_2$. These salts of $Cl^-$, $Mg^{2+}$, and $K^+$ are directly emitted in atmosphere and are water soluble in nature. Many sulfate salts of calcium and magnesium are used in fireworks to introduce color and brightness which are eventually responsible for high $SO_2$, $Ca^{2+}$, and $Mg^{2+}$ ions in aerosols.

Second, the higher aerosol mass and soluble ion concentrations are linked not only to their direct emissions but also to their restricted vertical dispersal after emission. The light energy released during firework displays changes the meteorological conditions which favors accumulations of particles and gaseous emissions near the surface and results in higher concentrations. The firework activity is known to affect the meteorological parameters such as temperature and relative humidity (Saha et al. 2014). Devara et al. (2015) have reported warming of +82 W m$^{-2}$ in the atmosphere during festival period. In the present work, it is important to note that the mixing height on the Diwali night reduced as low as 50 mts compared to before (227 mts) and after (269 mts) Diwali period (Table 1). Temperature inversions conditions and lowering of mixing height are frequent natural phenomenon in this region but during extreme winters not during Diwali festival period. Here, we suggest that the lowering

of mixing height is induced by firework displays. The light emitted during firework displays in Delhi has been observed to have wavelength less than 242 nm and was enough to break molecular oxygen (Attri et al. 2001). This could lead to the warming of ambient atmosphere near the surface as has also been reported by Devara et al. (2015). Since the surface remained cooler and sudden increase in temperature near the surface lead to temperature inversion conditions (by definition), the height at which the temperature increased became the mixing height as it acted as barrier for air to rise and pollutants to disperse (Fig. 5). The burning of firecrackers emits large amount of soot particles and metal oxide in the size range of less than 1 μm (Prakash et al. 2013), which accumulate in ambient atmosphere under the firework activity induced inversion conditions.

Third, the high energy light could lead to formations of secondary pollutants (Attri et al. 2001; Jiang et al. 2015). The higher concentrations of $NO_3^-$, $SO_4^{2-}$, and $NH_4^+$ are attributed to the presence of precursor gases such as $SO_2$, $NO_2$, $NH_3$, light energy, and the humidity. The water molecules, one of the end products in firework burning, get concentrated in ambient atmosphere as the water vapor holding capacity of hot air increases (Ganguly 2015; Devara et al. 2015). Based on this, we suggest that both gas phase and aqueous phase photochemical reactions lead to formation of secondary pollutants. The calcium and magnesium salts produced $SO_2$ which eventually gets oxidizes to $SO_4^{2-}$ due to photochemical processes. This transformation is accelerated by Fe content emitted during firework displays (Chatterjee et al. 2013), not analyzed in this work. The aqueous phase transformation of $SO_2$ into $SO_4^{2-}$ is facilitated by $H_2O_2$. The hydrogen peroxide is formed by chain terminating steps of $OH_2$ radicals. The possible pathways can be written as follows:

$$O_2 \xrightarrow{< 242\ nm} O$$
$$O_2 + O \rightarrow O_3$$
$$O_3 \xrightarrow{light} O^1D_2 + O_2$$
$$O^1D_2 + H_2O \rightarrow 2OH$$
$$OH + NO_2 \rightarrow NO + HO_2$$
$$H_2O + HO_2 \rightarrow H_2O_2 + O_2$$
$$H_2O_2 + SO_2 \rightarrow H_2SO_4 \text{———————aqueous phase reaction}$$
$$NO \xrightarrow{light + VOCs, CO,\ CH_4} NO_2$$
$$NO_2 + O_3 \rightarrow NO_3 + O2$$
$$NO_3 + NO \rightarrow 2NO_2$$
$$NO_3 + NO_2 \rightarrow N_2O_5$$

The conversion of ammonia to ammonium ions has been previously reported by Kumar and Yadav (2016) in $PM_{10}$ aerosols in this region on account of emissions of ammonia from livestock, fertilizer applications, vehicular emissions (during reduction of NOx to molecular $N_2$), and the favorable meteorological conditions. The increments in amounts of aerosols and the soluble ions concentrations during AF period are due to the uplifting of the fine aerosols deposited during the preceding night by large-scale citywide sweeping activity as discussed before. In addition $CaCO_3$, $CaSO_4$, and $Ca(NO_3)_2$ are the dominant chemical forms in the desert dust particles (Radhi et al. 2010), which are abundantly available in this region (Yadav and Rajamani 2004, 2006) and undergo resuspension. The heterogeneous mineral dust mediated reactions of $SO_2$ and NOx, emitted directly from firework, such as replacement of $Cl^-$ by $NO_3^-$, and $SO_4^{2-}$, coating of $NO_3^-$ and $SO_4^{2-}$ on soot, and formation of secondary organic aerosols are the main aging mechanisms of firework induced particles (Kong et al. 2015) and responsible for high concentration of SIA after firework display.

## Conclusions

The widespread firework displays during Diwali festival is responsible for higher aerosol's mass concentrations in the ambient atmosphere. This activity contributes more aerosols in $PM_{0.95}$ fractions and raised the mass concentrations to 786 μg m$^{-3}$ compared to 40 μg m$^{-3}$ limit for $PM_{2.5}$ as per NAAQS in India. The alveolar, respirable, and inhalable fractions accounted for 64.6, 90.8, and 97.8 %, respectively, of the total $PM_{10}$ mass. The concentrations of aerosol's mass and most of WSII were highest in $PM_{0.95}$ and decreased with increase in particle size during firework displays. The mass concentration of $Mg^{2+}$, $Cl^-$, and $K^+$ (markers for firework) shows 147.7, 89.5, and 26.3 times higher value, respectively, in $PM_{0.95}$ during Diwali period compared to before Diwali period.
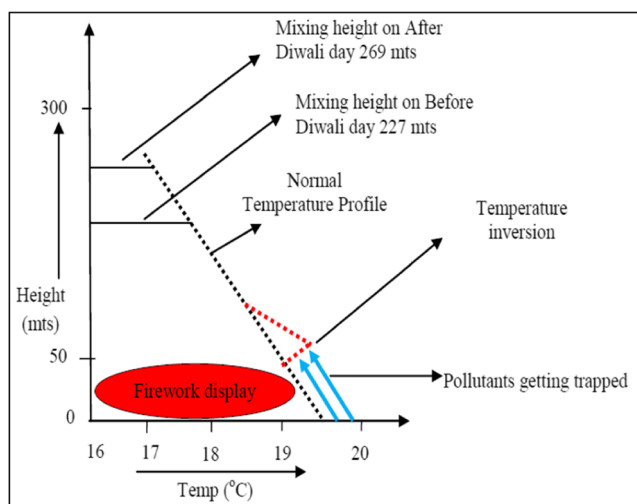


**Fig. 5** Demonstrative graph explaining firework-induced temperature inversion condition in ambient atmosphere (the height of temperature inversion becomes the mixing height)

The firework contributes more OC compared to EC to the TC, and among different carbon fractions, OC2, OC3, and EC1 are dominant contributions. The high $Cl^-/Na^+$ (5.6) and high OC/EC (3.4) ratios of $PM_{0.95}$ can be used as the tracers for firework displays. The firework displays also induce the temperature inversion conditions and reduced the mixing height as low as 50 mts in comparison 227 and 269 mts during BF and AF periods, respectively. This phenomenon helps in accumulations of airborne fine particles and gaseous constituents near the surface. Firework displays also facilitated the gas phase and aqueous phase photochemical reactions for the formation of secondary pollutants. The study indicated that firework displays directly and indirectly influence the mass concentrations and soluble ion and carbon contents of ambient size-segregated aerosols. This activity is expected to have severe health impacts during the small time of direct exposure. Hence, public opinion against firework displays during festival seasons must be evolved to safeguard human health.

# References

Ambade B, Ghosh S (2013) Characterization of PM10 in the ambient air during Deepawali festival of Rajnandgaon district, India. Nat Hazards 69:589–598

Arimoto R, Duce RA, Savoie DL, Prospero JM, Talbot R, Cullen JD, Tomza U, Lewis NF, Jay BJ (1996) Relationships among aerosol constituents from Asia and the North Pacific during PEM–West A. J Geophys Res-Atmos 101:2011–2023

Attri AK, Kumar U, Jain VK (2001) Microclimate: formation of ozone by fireworks. Nature 411:1015. doi:10.1038/35082634

Cao JJ, Lee SC, Chow JC, Watson JG, Ho KF, Zhang RJ, Jin ZD, Shen ZX, Chen GC, Kang YM, Zou SC, Zhang LZ, Qi SH, Dai MH, Cheng Y, Zou SC (2007) Spatial and seasonal distributions of carbonaceous aerosols over China. J Geophys Res-Atmos 112(D22)

Cao J, Lee S, Ho K, Zhang X, Zou S, Fung K, Chow J, Watson J (2003) Characteristics of carbonaceous aerosol in Pearl River Delta region, China during 2001 winter period. Atmos Environ 37:1451–1460

Chatterjee A, Sarkar C, Adak A, Mukherjee U, Ghosh SK, Raha S (2013) Ambient air quality during Diwali Festival over Kolkata—a Mega-City in India. Aerosol Air Qual Res 13:1133–1144

Chow JC, Watson JG, Chen LWA, Chang MCO, Robinson NF, Trimble D, Kohl SD (2007) The IMPROVE a temperature protocol for thermal/optical carbon analysis: maintaining consistency with a long-term database. J Air Waste Manage Assoc 57:1014–1023

Deka P, Hoque RR (2014) Diwali fireworks: early signs of impact on PM10 properties of rural Brahmaputra valley. Aerosol Air Qual Res 14:1752–1762

Do T, Wang C, Hsieh Y, Hsieh H (2012) Metals present in ambient air before and after a firework festival in Yanshui, Tainan, Taiwan. Aerosol Air Qual Res 12:981–993

Devara PCS, Vijayakumar K, Safai PD, Raju MP, Rao PSP (2015) Celebration-induced air quality over a tropical urban station, Pune, India. Atmos Pollu Res 6:511–520

Drewnick F, Hings SS, Cutius J, Eerdekens G, Williams J (2006) Measurement of fine particulate matter and gas-phase species during the New Year's fireworks 2005 in Mainz, Germany. Atmos Environ 40:4316–4327

Economic Survey of Delhi 2012-2013 (http://www.delhi.gov.in/wps/wcm/connect/doit_planning/Planning/Economic+Survey+of+Delhi/Economic+Survey+of+Delhi+2012+-+2013) assessed on 2nd January 2016

Feng J, Sun P, Hu XL, Zhao W, Wu MH, Fu JM (2012) The chemical composition and sources of PM2.5 during the 2009 Chinese New Year's holiday in Shanghai. Atmos Res 118:435–444

Gargava P, Chow JC, Watson JG, Lowenthal DH (2014) Speciated PM10 emission inventory for Delhi, India. Aerosol Air Qual Res 14:1515–1526

Ganguly DN (2015) Short term change in relative humidity during festival of Diwali in India. J Atmos Solar-Terrest Phy 129:49–54

Han YM, Lee SC, Cao JJ, Ho KF, An ZS (2009) Spatial distribution and seasonal variation of char-EC and soot-EC in the atmosphere over China. Atmos Environ 43:6066–6073

Hirai K, Yamazaki Y, Okada K, Furuta S, Kubo K (2000) Acute eosinophilic pneumonia associated with smoke from fireworks. Intern Med (Japan) 39:401–403

Jiang Q, Sun YL, Wang Z, Yin Y (2015) Aerosol composition and sources during the Chinese Spring Festival: fireworks, secondary aerosol, and holiday effects. Atmos Chem Phys 15:6023–6034

Joly A, Smargiassi A, Kosatsky T, Fournier M, Dabek-Zlotorzynska E, Celo V, Mathieu D, Servranckx R, D'amours R, Malo A, Brook J (2010) Characterisation of particulate exposure during fireworks displays. Atmos Environ 44:4325–4329

Kiss G, Varga B, Galambos I, Ganszky I (2002) Characterization of water-soluble organic matter isolated from atmospheric fine aerosol. J Geophys Res 107(D21):8339. doi:10.1029/2001JD000603

Kong SF, Li L, Li XX, Yin Y, Chen K, Liu DT, Yuan L, Zhang YJ, ShanYP JYQ (2015) The impacts of firework burning at the Chinese Spring Festival on air quality: insights of tracers, source evolution and aging processes. Atmos Chem Phys 15:2167–2184

Kumar P, Yadav S (2013) Factors and sources influencing ionic composition of atmospheric condensate during winter season in lower troposphere over Delhi India. Environ Monit Assess 185:2795–2805

Kumar P, Yadav S (2016) Seasonal variations in water soluble inorganic ions, OC and EC in PM10 and PM >10 aerosols over Delhi: influence of sources and meteorological factors. Aerosol Air Qual Res 16:1165–1178

Kumar P, Yadav S, Kumar A (2014) Sources and processes governing rainwater chemistry in New Delhi, India. Nat Hazards 74:2147–2162

Limaye S, Salvi S (2010) Ambient air pollution and the lungs: what do clinicians need to know? Breathe 6:235–244

Mandal P, Prakash M, Bassin JK (2012) Impact of Diwali celebrations on urban air and noise quality in Delhi City, India. Environ Monit Assess 184:209–215

Nirmalkar J, Deb MK, Deshmukh DK, Verma SK (2013) Mass loading of size segregated atmospheric aerosols in the ambient air during fireworks episodes in eastern central India. Bull Environ Contam Toxicol 90:434–439

Nishanth T, Praseed KM, Rathnakaran K, Kumar MKS, Krishna RR, Valsaraj KT (2012) Atmospheric pollution in a semi-urban, coastal region in India following festival seasons. Atmos Environ 47:295–306

O'Shaughnessy PT, Raabe OG (2003) A comparison of cascade impactor data reduction methods. Aerosol Sci Technol 37(2):187–200

Perrino C, Tiwari S, Catrambone M, Torre SD, Rantica E, Canepari S (2011) Chemical characterization of atmospheric PM in Delhi,

India, during different periods of year including Diwali Festival. Atmos Pollut Res 2:418–427

Prakash D, Payra S, Verma S, Soni M (2013) Aerosol particle behavior during dust storm and Diwali over an urban location in north western India. Nat Hazards 69:1767–1779

Radhi M, Box MA, Box GP, Mitchell RM, Cohen DD, Stelcer E, Keywood MD (2010) Optical, physical and chemical characteristics of Australian continental aerosols: results from a field experiment. Atmos Chem Phys 10(13):5925–5942

Saha U, Talukdar S, Jana S, Maitra A (2014) Effects of air pollution on meteorological parameters during Deepawali festival over an Indian urban metropolis. Atmos Environ 98:530–539

Ravindra K, Mor S, Kaushik CP (2003) Short-term variation in air quality associated with firework events: a case study. J Environ Monit 5:260–264

Sarkar S, Khillare PS, Jyethi DS, Hasan A, Parween M (2010) Chemical speciation of respirable suspended particulate matter during a major firework festival in India. J Hazard Mater 184:321–330

Singh RP, Kaskaoutis DG (2014) Crop residue burning: a threat to South Asian air quality. Eos 95:333–340

Tandon A, Yadav S, Attri AK (2008) City wide sweeping a source for respirable particulate matter in the atmosphere. Atmos Environ 42: 1064–1069

Tandon A, Yadav S, Attri AK (2010) Coupling between meteorological factors and ambient aerosol load. Atmos Environ 44:1237–1243

Tiwari S, Chate DM, Srivastava MK, Safai PD, Bisht DS (2012) Statistical evaluation of PM10 and distribution of PM1, PM2.5 and PM10 in ambient air due to extreme fireworks episodes (Deepawali festivals) in megacity Delhi. Nat Hazards 61:521–531

Tsai HH, Chien LH, Yuan CS, Lin YC, Jen YH, Ie IR (2012) Influences of fireworks on chemical characteristics of atmospheric fine and coarse particles during Taiwan's Lantern Festival. Atmos Environ 62:256–264

Turpin BJ, Lim HJ (2001) Species contributions to PM2.5 mass concentrations: revisiting common assumptions for estimating organic mass. Aerosol Sci Technol 35:602–610

Vecchi R, Bernardoni V, Cricchio D, Alessandro AD, Fermo P, Lucarelli F, Nava S, Piazzalunga A, Valli G (2008) The impact of fireworks on airborne particles. Atmos Environ 42:1121–1132

Wang Y, Zhuang GS, Xu C, An ZS (2007) The air pollution caused by the burning of fireworks during the lantern festival in Beijing. Atmos Environ 41:417–431

Yadav S, Kumar P (2014) Pollutant scavenging in dew water collected from an urban environment and related implications. Air Qual Atmos Health 7:559–566

Yadav S, Rajamani V (2004) Geochemistry of aerosols of northwestern part of India adjoining the Thar Desert. Geochim Cosmochim Acta 68:1975–1988

Yadav S, Rajamani V (2006) Air quality and trace metal chemistry of different size fractions of aerosols in N–NW India—implications for source diversity. Atmos Environ 40:698–712

Yadav S, Tandon A, Tripathi JK, Yadav S, Attri AK (2016) Statistical assessment of respirable and coarser size ambient aerosol sources and their timeline trend profile determination: a four year study from Delhi. Atmos Pollut Res 7:190–200

Yang L, Gao X, Wang X, Nie W, Wang J, Gao R, Xu P, Shou Y, Zhang Q, Wang W (2014) Impacts of firecracker burning on aerosol chemical characteristics and human health risk levels during the Chinese New Year Celebration in Jinan, China. Sci Total Environ 476:57–64

Yttri KE, Aas W, Bjerke A, Cape JN, Cavalli F, Ceburnis D, Dye C, Emblico L, Facchini MC, Forster C, Hanssen JE, Hansson HC, Jennings SG, Maenhaut W, Putaud JP, Tørseth K (2007) Elemental and organic carbon in PM10: a one year measurement campaign within the European Monitoring and Evaluation Programme EMEP. Atmos Chem Phys 7:5711–5725

Zhao S, Yu Y, Yin D, Liu N, He J (2014) Ambient particulate pollution during Chinese Spring Festival in urban Lanzhou, Northwestern China. Atmos Pollut Res 5:335–343